Spin and charge transport in double-junction Fe/MgO/GaAs/MgO/Fe heterostructures

S. Wolski,[1,a)] T. Szczepański,[1] V. K. Dugaev,[1,2] J. Barnaś,[3,4] B. Landgraf,[5] T. Slobodskyy,[5] and W. Hansen[5]

[1]*Department of Physics, Rzeszów University of Technology, Al. Powstańców Warszawy 6, 35-959 Rzeszów, Poland*
[2]*Departamento de Física and CFIF, Instituto Superior Técnico, Universidade de Lisboa, Av. Rovisco Pais, 1049-001 Lisbon, Portugal*
[3]*Faculty of Physics, Adam Mickiewicz University, ul. Umultowska 85, 61-614 Poznań, Poland*
[4]*Institute of Molecular Physics, Polish Academy of Sciences, Smoluchowskiego 17, 60-179 Poznań, Poland*
[5]*Institute for Applied Physics, University of Hamburg, Jungiusstraße 11, 20355 Hamburg, Germany*

(Received 1 December 2014; accepted 7 January 2015; published online 27 January 2015)

We present theoretical and experimental results on tunneling current in single Fe/MgO/GaAs and double Fe/MgO/GaAs/MgO/Fe tunnel junctions. The charge and spin currents are calculated as a function of external voltage for different sets of parameters characterizing the semiconducting GaAs layer. Transport characteristics of a single Fe/MgO/GaAs junction reveal typical diode as well as spin diode features. The results of numerical calculations are compared with current-voltage characteristics measured experimentally for double tunnel junction structures, and a satisfactory agreement of the theoretical and experimental results has been achieved. © *2015 AIP Publishing LLC*. [http://dx.doi.org/10.1063/1.4906397]

I. INTRODUCTION

One of the most important issues in modern spintronics is the problem of effective spin injection from a ferromagnetic metal into a nonmagnetic semiconductor through an insulating tunnel barrier.[1,2] The efficiency of direct spin injection from a ferromagnet into a semiconductor is usually strongly suppressed[3,4] due to a large mismatch between electrical conductivities of metals and semiconductors.[5] The presence of a barrier is thus crucial as it provides a way to achieve relatively large spin polarization of injected electrons.[6–11]

To optimize transport characteristics of ferromagnet-semiconductor tunnel junctions, one needs to develop reliable models and methods of computer simulations of the spin and charge transfer in tunnel junctions, taking into account different mechanisms of electron transport. In principle, the main mechanisms, such as direct tunneling of electrons, thermally activated electron jump, mixed tunneling-activation jump, and the electric-field activated current (Poole-Frenkel effect), have been thoroughly studied in the past (see, e.g., Refs. 12–19 and the literature therein).

The problem, however, is still far from being fully understood and solved. The main difficulties in the theoretical description and numerical calculations of the tunneling current arise from the fact that such calculations cannot be easily combined with the semiclassical approach to transport in semiconductor-based heterojunctions. Moreover, the electron tunneling in a ferromagnet/oxide/semiconductor structure cannot be simply described by textbook formulae because of uncertainty concerning not only some parameters describing real structure of the barrier but also wavefunctions and spin polarization of electrons near interfaces. All this is especially important for the calculation of spin-resolved current-voltage (I-V) characteristics, when the deviation from equilibrium is not very small. It should be also noted that in real tunnel structures, one has to take into account atomic structure of real interfaces and the presence of defects, which unavoidably affect electronic and magnetic properties near/within the barrier.

In this paper, we concentrate mainly on the tunneling mechanism of electron transport through the barrier, assuming that the barrier is rather high, so that the voltage drop appears mainly at the insulating barrier. This is the case for MgO insulating barrier separating Fe ferromagnet and GaAs semiconductor. The estimations show that for the Fe/MgO/GaAs structure, this mechanism prevails at not very high temperatures (e.g., below the room temperature). In such a case, shape of the voltage-current characteristics is determined mainly by the band offset of GaAs with respect to Fe, which, in turn, is determined by the doping level of the GaAs semiconductor. The most important problem for the I–V characteristics is the variation of the barrier shape with the bias voltage, and the corresponding variation of the electronic structure in the semiconductor with respect to the energy bands in the ferromagnet.

Transport characteristics have been also measured experimentally on double-barrier tunnel heterostructures. The junctions include Fe disks deposited on the surface of the GaAs semiconductor and then covered with a thin MgO insulating layer. We show that our theoretical and numerical results are in a satisfactory agreement with the experimentally measured current-voltage characteristics.

The outline of the paper is as follows: In Sec. II, we describe the model and also present basic theoretical background. In Sec. III, we consider charge and spin transport in a double barrier junction. Both fast and slow spin relaxation

[a)]Electronic address: wolski@prz.edu.pl

limits in the GaAs layer are considered there. Comparison with experimentally measured transport characteristics is presented in Sec. IV, while summary and final conclusions are in Sec. V.

II. MODEL

We consider first a single Fe/MgO/GaAs heterojunction. The electronic energy structure of such a junction is presented schematically in Fig. 1(a) for the case of zero bias voltage, $V=0$, and in Fig. 1(b) for a relatively large voltage, $V>0$. Note that according to our definition, positive voltage corresponds to the electrostatic potential of the GaAs electrode higher than that of the Fe electrode, so positive current flows from right to left (from GaAs to Fe). The energy in Fig. 1 is measured from the Fermi level in Fe (the left electrode), so that we put $\varepsilon_F=0$. We assume that the electrochemical potential μ of the right electrode (corresponding to GaAs) is located in the semiconductor energy gap. This corresponds to the case of a non-degenerate weakly doped GaAs, and the relative location of the chemical potential with respect to the conduction and valence band edges, ε_c and ε_v, respectively, is solely determined by the GaAs doping and by temperature. The parameters ε_{c0} and ε_{v0} describe position of the corresponding conduction and valence band edges at zero bias, $V=0$. Accordingly, the semiconductor energy gap is $\varepsilon_g=\varepsilon_{c0}-\varepsilon_{v0}$. When the bias voltage is nonzero, $V\neq 0$, one finds $\varepsilon_c=\varepsilon_{c0}-eV$, $\varepsilon_v=\varepsilon_{v0}-eV$, and the electrochemical potential for electrons in the semiconductor is $\mu=-eV$. Here, e is the absolute value of electron charge ($e>0$).

In Fig. 1, we have not shown the energy-band bending in the semiconducting GaAs. Strictly speaking, such a band bending is always present near the MgO/GaAs interface, but in our description, it may be neglected, since we assume that the electric current is determined mainly by tunneling through the MgO barrier.

As shown in Fig. 1, the effective height of the MgO tunnel barrier measured from the band bottom in Fe is different

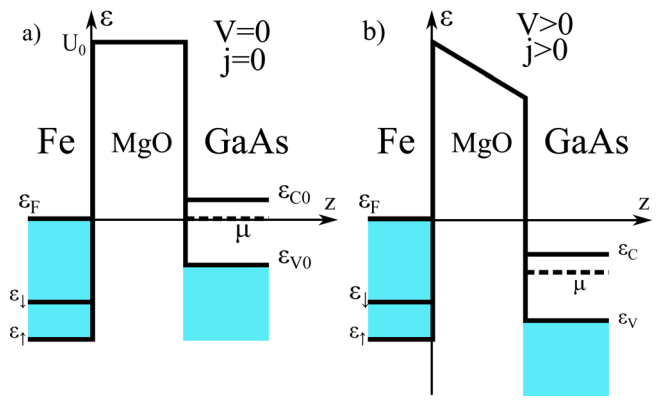

FIG. 1. Schematic view of the energy band diagram for a model metal-insulator-semiconductor (MIS) heterostructure. The energy is measured from the Fermi level in the left (Fe) electrode. The electrochemical potential in the right electrode (GaAs) is denoted by μ. Bottom edges of the spin-majority and spin-minority electron bands in Fe are $\varepsilon_\uparrow$ and $\varepsilon_\downarrow$, respectively. The bottom (top) conduction (valence) band edge is denoted as ε_{c0} (ε_{v0}) for zero bias and ε_c (ε_v) for a finite bias voltage. Barrier height measured from the Fermi level in Fe is denoted by U_0.

for the spin-majority and spin-minority electrons, which is due to the strong spin splitting of the electron band in Fe—the relevant band edges for the spin-majority and spin-minority electrons are denoted as $\varepsilon_\uparrow$ and $\varepsilon_\downarrow$, see Fig. 1. Apart from this, the electronic states in the MgO barrier, which couple to the spin-majority and spin-minority states of the Fe electrode, have different symmetries and also different attenuation factors in the MgO barrier.[20,21] All this leads to a significant spin filtering properties of the MgO barrier and large tunnel magnetoresistance (TMR) in MgO-based tunnel junctions.[22,23,25]

Density of the electron and hole tunneling currents in the spin-σ channel can be calculated for $V>0$ as

$$j_{e\sigma}(V>0)=\frac{e\sqrt{m}}{4\pi^2\hbar\sqrt{m_e}}\int_{\varepsilon_c}^{\infty}d\varepsilon\int_0^{\sqrt{2m_e(\varepsilon-\varepsilon_c)}/\hbar}k_l dk_l \times|t_{\mathbf{k}e\sigma}|^2\left(\frac{\varepsilon-\hbar^2k_l^2/2m_e-\varepsilon_c}{\varepsilon-\hbar^2k_l^2/2m-\varepsilon_\sigma}\right)^{1/2}\left[f^L(\varepsilon)-f^R(\varepsilon)\right], \tag{1}$$

$$j_{h\sigma}(V>0)=\frac{e\sqrt{m}}{4\pi^2\hbar\sqrt{m_h}}\int_{-\infty}^{\varepsilon_v}d\varepsilon\int_0^{\sqrt{2m_h(\varepsilon_v-\varepsilon)}/\hbar}k_l dk_l \times|t_{\mathbf{k}h\sigma}|^2\left(\frac{\varepsilon_v+\hbar^2k_l^2/2m_h-\varepsilon}{\varepsilon-\hbar^2k_l^2/2m-\varepsilon_\sigma}\right)^{1/2}\left[f^L(\varepsilon)-f^R(\varepsilon)\right], \tag{2}$$

respectively, where k_l is the in-plane wavevector component for an electron incident from Fe at the Fe/MgO interface, $|t_{\mathbf{k}e\sigma}|^2$ and $|t_{\mathbf{k}h\sigma}|^2$ are the transmission coefficients of electrons and holes with spin σ, whereas m, m_e, and m_h are the effective masses of electrons in Fe, electrons in GaAs, and holes in GaAs, respectively. The Fermi-Dirac distribution functions for the left and right electrode are denoted as $f^L(\varepsilon)=(e^{\beta\varepsilon}+1)^{-1}$ and $f^R(\varepsilon)=(e^{\beta(\varepsilon-\mu)}+1)^{-1}$, respectively, with $\beta=1/k_BT$.

The transmission coefficients in Eqs. (1) and (2) can be calculated as

$$|t_{\mathbf{k}}|^2=\frac{16\gamma k_L^2\kappa_R\kappa_L m_e^2}{(k_Lk_Rm-\kappa_L\kappa_Rm_e)^2g_-+(k_Lk_Rm+k_R\kappa_Lm_e)^2g_+}, \tag{3}$$

where

$$g_\pm=\left[\exp\left(\int_0^{L_b}\kappa(z)\,dz\right)\pm\exp\left(-\int_0^{L_b}\kappa(z)\,dz\right)\right]^2, \tag{4}$$

and k_L and k_R are the wavevector components normal to the barrier in the left and right electrodes, respectively. Apart from this, $i\kappa(z)$ is the semiclassical imaginary wavevector component corresponding to the subbarrier motion of an electron or a hole, and is determined by the barrier height U_0 (see Fig.1) and voltage. Apart from this, $\kappa_L=\kappa(0)$ and $\kappa_R=\kappa(L_b)$, while L_b is the width of the tunnel barrier.

In Eq. (3), we introduced a phenomenological factor $\gamma\leq 1$ to take into account peculiarity of the transmission of majority and minority electrons through the Fe/MgO

interface. The model with $\gamma = 1$ describes tunneling through the barrier in the approximation of free electron waves penetrating from the Fe electrode to the MgO insulator. As follows from *ab initio* calculations,[20,21] the wave functions of majority and minority electrons in Fe decay differently in the MgO insulator. Correspondingly, the TMR of epitaxial Fe/MgO/Fe tunnel junction can be as high as 1000% or even more. It turns out that in real structures, TMR of up to 400% can be observed.[22,23] The value of TMR can be, however, much lower when the Fe/MgO interface has structural defects and/or ill-controlled overlayers like FeO interfacial layer for instance (see discussion in Ref. 24).

In our calculations, we assumed $\gamma = 0.3$, which corresponds to TMR of about 100% for the Fe/MgO/Fe tunnel junction. This is demonstrated in Fig. 2, where the numerical results are presented for $\gamma = 0.3$ and $\varepsilon_\uparrow = -4.5\,\mathrm{eV}$ ($\varepsilon_\downarrow = -3\,\mathrm{eV}$) for the spin-majority (spin-minority) electrons in Fe.

As already mentioned above, Eqs. (1)–(3) correspond to the case of $V > 0$, shown schematically in Fig. 1. In the opposite case, $V < 0$, when the electrons flow from GaAs to the Fe electrode, one finds

$$j_{e\sigma}(V<0) = \frac{e\sqrt{m_e}}{4\pi^2\hbar\sqrt{m}} \int_{\varepsilon_c}^{\infty} d\varepsilon \int_0^{\sqrt{2m_e(\varepsilon-\varepsilon_c)}/\hbar} k_l dk_l \times |t_{\mathbf{k}e\sigma}|^2 \left(\frac{\varepsilon - \hbar^2 k_l^2/2m - \varepsilon_\sigma}{\varepsilon - \hbar^2 k_l^2/2m_e - \varepsilon_c} \right)^{1/2} \left[f^L(\varepsilon) - f^R(\varepsilon) \right], \tag{5}$$

$$j_{h\sigma}(V<0) = \frac{e\sqrt{m_h}}{4\pi^2\hbar\sqrt{m}} \int_{-\infty}^{\varepsilon_v} d\varepsilon \int_0^{\sqrt{2m_h(\varepsilon_v-\varepsilon)}/\hbar} k_l dk_l \times |t_{\mathbf{k}h\sigma}|^2 \left(\frac{\varepsilon - \hbar^2 k_l^2/2m - \varepsilon_\sigma}{\varepsilon_v + \hbar^2 k_l^2/2m_h - \varepsilon} \right)^{1/2} \left[f^L(\varepsilon) - f^R(\varepsilon) \right] \tag{6}$$

with

$$|t_{\mathbf{k}}|^2 = \frac{16\gamma k_R^2 \kappa_R \kappa_L m^2}{(k_L k_R m - \kappa_L \kappa_R m_e)^2 g_- + (k_L \kappa_R m_e + k_R \kappa_L m)^2 g_+}. \tag{7}$$

The total density of electric current flowing through the junction is the sum of partial currents due to holes and electrons flowing in both spin channels

$$j = \sum_{l\sigma} j_{l\sigma}, \tag{8}$$

where $l = e, h$. Correspondingly, the total spin current can be calculated as the difference between the spin-up and spin-down currents in both electron and hole channels

$$J^s = \frac{1}{e} \sum_l (j_{l\uparrow} - j_{l\downarrow}). \tag{9}$$

The latter definition corresponds to the number of 1/2-spins transferred through a unit area of the junction per unit time. The results of numerical calculations of the charge and spin currents for a single Fe/MgO/GaAs junction are presented in Figs. 3 and 4 as a function of voltage V, and for different values of the conduction band edge ε_{c0}. As one can see, the current-voltage characteristics reveal typical diode behavior, with a large asymmetry between positive and negative voltages. This asymmetry is due to the asymmetrical position of the Fermi level in GaAs at zero bias with respect to the band edges ε_{c0} and ε_{v0}. Such an asymmetry also holds for the spin current. Thus, the junction can work as conventional as well as spin diode. As we see, both the charge and spin currents increase when ε_{c0} decreases (this corresponds to increasing doping of GaAs by donor impurities).

III. CHARGE AND SPIN TRANSPORT IN DOUBLE Fe/MgO/GaAs/MgO/Fe TUNNEL JUNCTIONS

Now we consider electronic and spin transport in the double-junction structure Fe/MgO/GaAs/MgO/Fe, with two

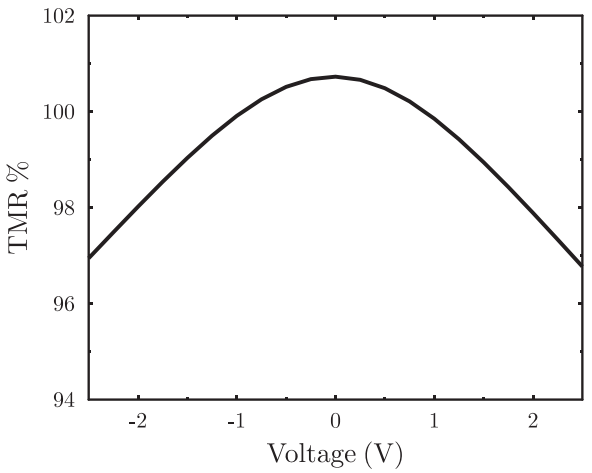

FIG. 2. TMR calculated for the Fe/MgO/Fe tunnel junction with $\gamma = 0.3$. Here, we use the parameters $m = m_0$ (m_0 is the free electron mass), $\varepsilon_\uparrow = -4.5\,\mathrm{eV}$, $\varepsilon_\downarrow = -3\,\mathrm{eV}$ for Fe, MgO barrier height $U_0 = 7.8\,\mathrm{eV}$, and barrier width $L_b = 1\,\mathrm{nm}$.

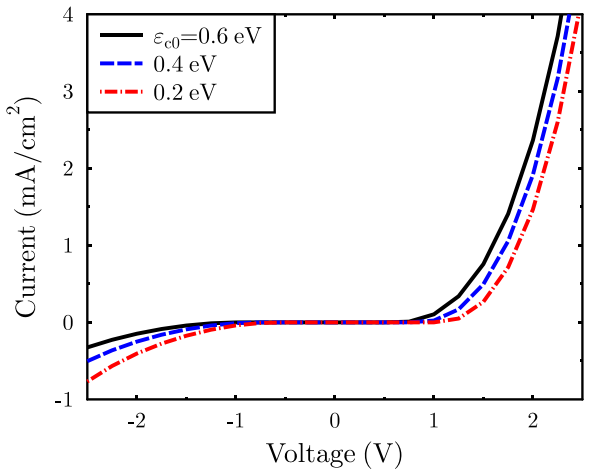

FIG. 3. Current-voltage characteristics of the Fe/MgO/GaAs junction, calculated for indicated values of the zero-bias conduction band edge and standard parameters of GaAs: $m_e = 0.066\ m_0$, $m_h = 0.085\ m_0$, energy gap $\varepsilon_g = 1.52\,\mathrm{eV}$. Other parameters as in Fig. 2.

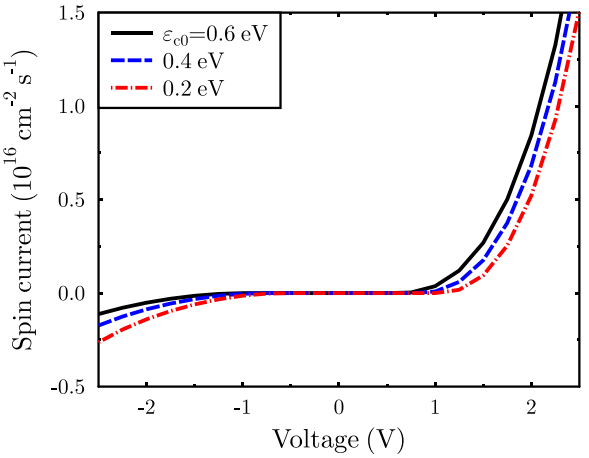

FIG. 4. Spin current vs. voltage in the Fe/MgO/GaAs junction, calculated for the same parameters as in Fig. 3.

MgO tunnel barriers, see Fig. 5. We consider two limiting situations: weak and strong spin relaxation in GaAs.

A. Weak spin relaxation in GaAs

We consider first the limit of very weak spin relaxation in the GaAs layer. This assumption applies to structures with sufficiently thin GaAs layers, $L_C \ll \ell_s$, where L_C is the thickness of the GaAs layer and ℓ_s is the spin relaxation length in GaAs. In such a situation, the current is conserved separately in each spin channel. This, in turn, means that we can still use Eqs. (1) and (2) to calculate the partial currents flowing through both barriers, but the location of the electrochemical potential in the GaAs layer should be determined from the condition of current conservation in the spin-up and spin-down channels separately. Moreover, since the resistance of both tunnel junctions depends on spin orientation, there is a spin splitting of the electrochemical potentials in GaAs, i.e., a nonequilibrium spin accumulation appears in the GaAs layer.

Accordingly, instead of $[f^L(\varepsilon) - f^R(\varepsilon)]$ in Eqs. (1) and (2), one should now use $[f^L(\varepsilon) - f^C_\sigma(\varepsilon)]$ when calculating the spin-σ current in the left junction, and $[f^C_\sigma(\varepsilon) - f^R(\varepsilon)]$ when calculating the spin-σ current in the right junction. Here, by $f^C_\sigma(\varepsilon) = (e^{\varepsilon-\mu_\sigma}+1)^{-1}$ we denoted the Fermi-Dirac distribution function of spin-σ electrons in GaAs, and μ_σ is the spin-dependent quasi-equilibrium electrochemical potential in GaAs.

The energy band diagram in the case of weak spin relaxation in GaAs (thin GaAs layer) is shown in Fig. 5. Assuming that the resistance of the GaAs layer is much smaller than the resistance of the MgO insulating layers, we may neglect any variation of the electrochemical potentials μ_σ across the GaAs layer.

The results of numerical calculations of the charge and spin currents flowing through the double tunnel junction for the parallel alignment of the magnetizations of both Fe electrodes are shown in Figs. 6 and 7, respectively. In the numerical calculations, we used the iteration procedure to reach the condition of current conservation in each spin channel, which includes electron and hole spin-polarized currents in GaAs. In turn, the voltages at the left and right barriers, V^L and V^R, can be determined according to the formulas

$$V^L = -\frac{\mu_\uparrow + \mu_\downarrow}{2e}, \tag{10}$$

$$V^R = \frac{\mu_\uparrow + \mu_\downarrow - 2\mu}{2e}, \tag{11}$$

where μ is the electrochemical potential in the right Fe electrode, while $(\mu_\uparrow + \mu_\downarrow)/2e$ is the average electrochemical potential in the central (GaAs) layer.

Since the double-junction structure is symmetrical, we show in Figs. 6 and 7 only one (positive) branch of the *I–V* characteristics. It is worth noting that independently of the bias polarization, one of the junctions is under the reverse bias, while the other one is under the forward bias. Consequently, the voltage drop at one of the barriers is much larger than that at the other barrier.

We have also calculated the charge and spin currents for the antiparallel magnetic configuration of the Fe layers, with the magnetic moment of the right Fe electrode reversed. The

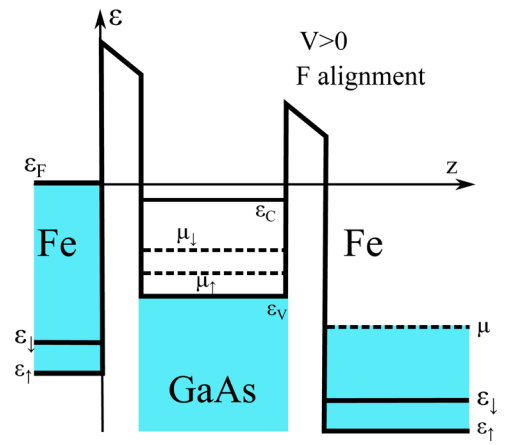

FIG. 5. Schematic energy band diagram of a double tunnel junction with parallel alignment of the magnetizations of both left and right Fe electrodes. The electrochemical potential in the GaAs layer is spin dependent due to spin accumulation.

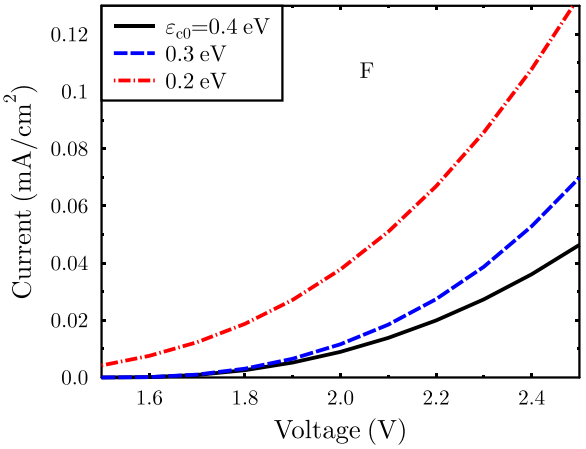

FIG. 6. Current-voltage characteristics of the double Fe/MgO/GaAs/MgO/Fe junction with a thin GaAs layer (weak spin relaxation in GaAs) for parallel (F) alignment of the magnetizations of both Fe electrodes. Parameters of GaAs, Fe, and the MgO barrier as in Fig. 3.

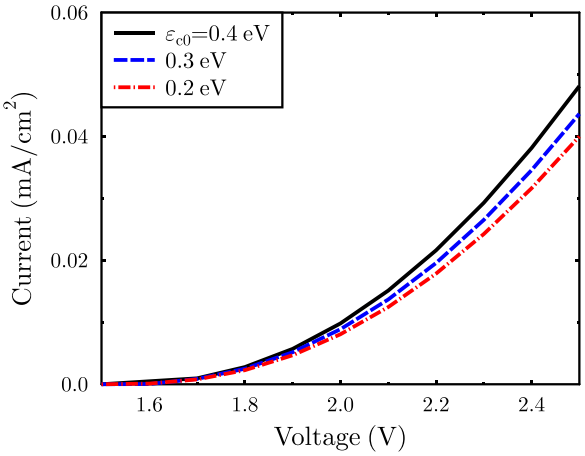

FIG. 7. Spin current vs bias voltage in the double Fe/MgO/GaAs/MgO/Fe junction for weak spin relaxation in the GaAs layer and for parallel (F) alignment of the magnetizations of both Fe electrodes. Other parameters as in Fig. 6.

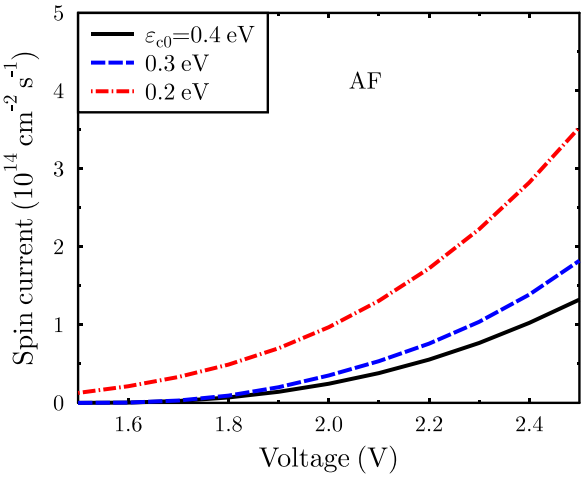

FIG. 9. Spin current vs bias voltage in the double Fe/MgO/GaAs/MgO/Fe junction with a thin GaAs layer (weak spin relaxation) for the antiparallel (AF) magnetic configuration of the Fe layers. Other parameters as in Fig. 6.

charge and spin currents in this configuration are shown in Figs. 8 and 9. As one can see in Figs. 6–9, the effect of parallel to antiparallel re-orientation on the charge and spin currents is about 20%.

B. Strong spin relaxation in GaAs

In the opposite limit of strong spin relaxation in GaAs layer, when the condition of $\ell_s \ll L_C$ is fulfilled, only the total charge current must be conserved, $j^L = j^R$, where $j^{L,R}$ is the sum of all partial currents in the left and right junctions. Correspondingly, we use now the model, in which the electrochemical potential in GaAs is the same for both spin orientations, $\mu_\uparrow = \mu_\downarrow = \mu_c$. This means that the spin splitting of electrochemical potential in the vicinity to the MgO/GaAs interfaces is negligibly small.

The dependence of charge and spin currents on the applied voltage in the double-junction structure with strong spin relaxation in GaAs is shown in Figs. 10 and 11, respectively. In the numerical calculations, we used now the iteration method to find self-consistently μ_c under the condition of the total current conservation. Note that there is now no dependence of the current on the relative alignment of the magnetizations of the left and right electrodes, i.e., the associated tunnel magnetoresistance vanishes exactly. This is because the spin memory is lost in the GaAs layer due to spin relaxation processes. It is remarkable that the dependence on ε_{c0} is rather weak in the case of strong spin relaxation, and both the charge and spin currents decrease with decreasing ε_{c0}.

From the above follows that the I–V and J^s–V characteristics of the double junction structure are sensitive to the spin relaxation in the semiconducting GaAs. This is due to the variation of relative voltages at left and right junctions with the variation of spin relaxation rate.

IV. COMPARISON WITH EXPERIMENTAL DATA

To compare our calculations with experiment,[25] we have fabricated a Fe/MgO/GaAs tunneling structure using molecular beam epitaxy at the University of Hamburg. After oxide desorption, a 500 nm GaAs channel with doping of

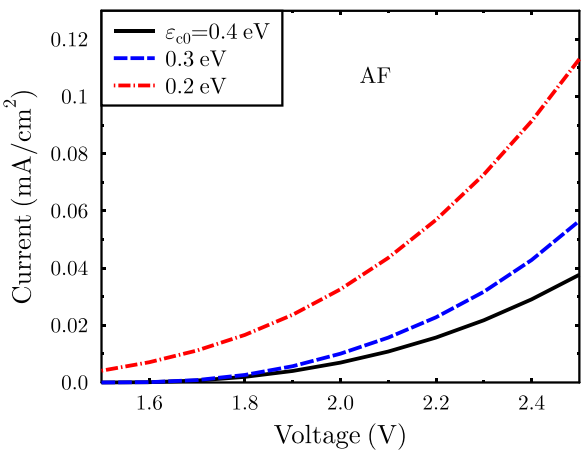

FIG. 8. Current-voltage characteristics of the double Fe/MgO/GaAs/MgO/Fe junction with a thin GaAs layer (weak spin relaxation in GaAs) for antiparallel (AF) alignment of the magnetization of both Fe electrodes. Other parameters as in Fig. 6.

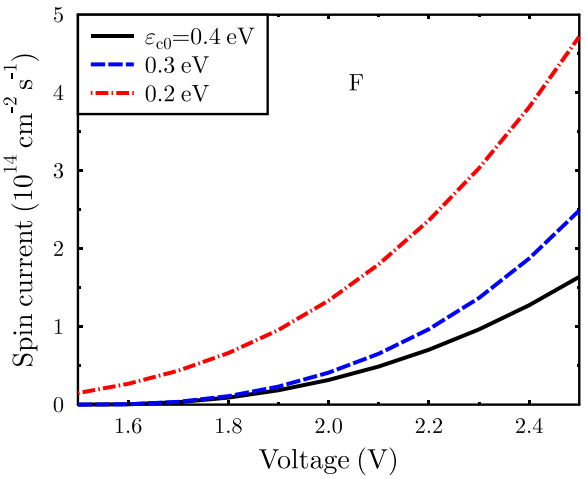

FIG. 10. Current-voltage characteristics of the double Fe/MgO/GaAs/MgO/Fe junction in the case of strong spin relaxation. Other parameters as in Fig. 6.

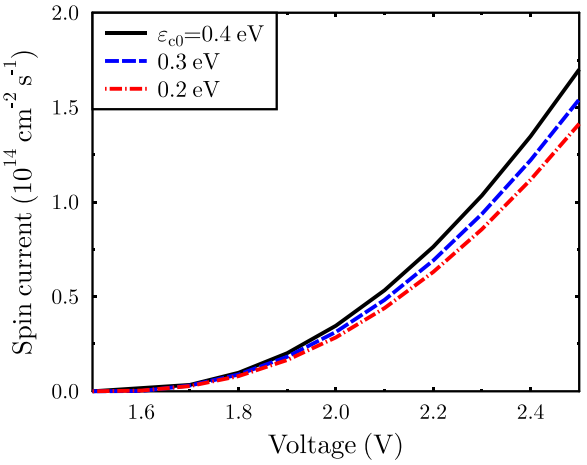

FIG. 11. Spin current vs. voltage in the double Fe/MgO/GaAs/MgO/Fe junction for strong spin relaxation. Other parameters as in Fig. 6.

$5 \times 10^{16}\,\mathrm{cm}^{-3}$ was deposited on an insulating GaAs(001) surface, which was followed by a 30 nm highly doped contact layer. Then, the sample was transferred to an oxide deposition chamber where a 5 nm thick MgO barrier was deposited. The sample transfer between the deposition chambers was performed in ultra-high vacuum assuring no contaminations at the interfaces. The structure was covered by a 6 nm Fe and a 10 nm gold films. The electrical measurements were performed on a structure with several MgO/Fe disks (see Fig. 12) at about 9 K using a closed cycle electro-transport cryostat, and in the two- and three-point measurements geometry. In each of them, the current-voltage characteristics (shown in Fig. 13) are related to the double oppositely-polarized junctions, which give the symmetric curve in the dependence on V_2.

Using Kirchhoff's laws, we can find the electric current vs voltage difference $V_2 - V_3$, which is basically the *I–V* characteristics of a single tunneling junction. The main parameters controlling the *I–V* characteristics are the barrier height and width, as well as the positions of the conduction and valence bands in GaAs with respect to the Fermi level in the Fe electrode (band offsets). We used Eqs. (1)–(6) to

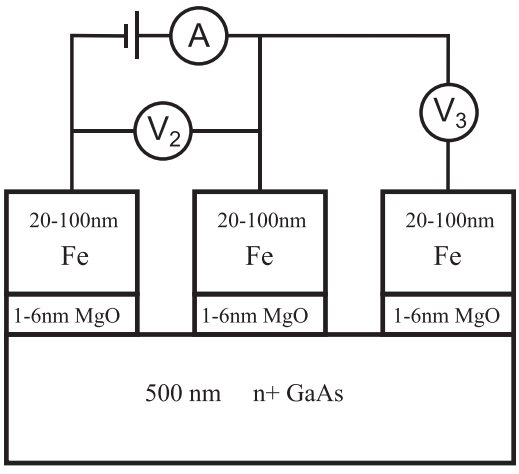

FIG. 12. Schematic view of the experimental setup with Fe/MgO/GaAs heterostructure for the two- and three-point measurements methods.

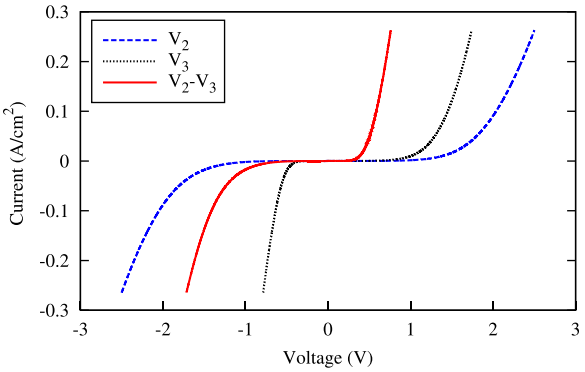

FIG. 13. Experimental *I–V* characteristics at $T = 8.967$ K for the MgO layer of 5 nm thick.

simulate the current-voltage characteristics and to determine the parameters which give the best fit of the experimental and theoretical data. Our results are presented in Fig. 14, where the current is the total current flowing through the system, i.e., it includes currents in all the channels. In general, it depends on the junction polarization and on the quasi-Fermi levels in the Fe electrode.

We have also performed the fitting procedure of the experimental data to our simulations in the model of the double tunnel junction, assuming $\ell_s \ll L$. We used the measurements of the reverse characteristics with the MgO thickness of $L_b = 6$ nm. As one can see in Fig. 15, the agreement with experiment is satisfactory. For low bias voltages, the agreement between theoretical and experimental curves is worse, which most probably is related to the effect of the drain through the third junction.

The spin current density, $J^s = (j_\uparrow - j_\downarrow)/e$, is shown in Fig. 16. The calculated spin polarization efficiency, defined as $p_s = (j_\uparrow - j_\downarrow)/(j_\uparrow + j_\downarrow)$, is almost constant, $p_s \approx 0.02$.

V. SUMMARY AND CONCLUSIONS

We have calculated numerically charge and spin tunneling current in heterostructures consisting of a single MgO tunnel barrier between ferromagnet (Fe) and semiconductor

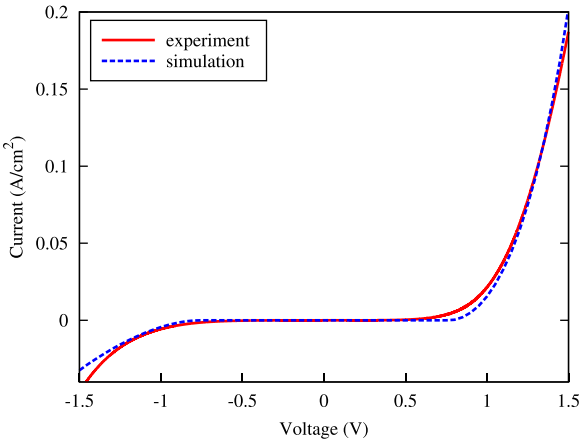

FIG. 14. Comparison of the experimental *I–V* characteristics with those obtained from numerical simulations. The parameters of simulation are barrier height $U_0 = 5.2$ eV, barrier width $L_b = 1.1$ nm, and the positions of conduction band edge $\varepsilon_{c0} = 0.76$ eV. Other parameters as in Fig. 6.

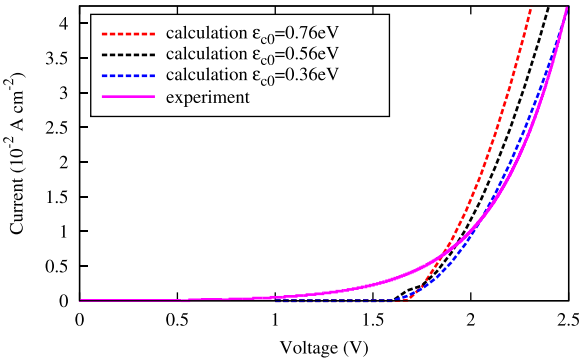

FIG. 15. Comparison of the experimental *I–V* characteristics with those obtained from numerical simulations for the double tunnel junction and for the parameters: barrier height $V_0 = 5.8$ eV, barrier width $L_b = 0.9$ nm (experiment 6 nm sample), and ε_{c0} as indicated. Other parameters as in Fig. 6.

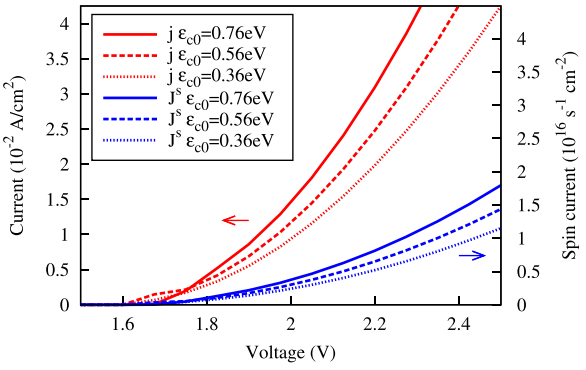

FIG. 16. Spin and electric current density characteristics for the best fitting parameters (barrier height $U_0 = 5.8$ eV and barrier width $L_b = 0.9$ nm). Other parameters as in Fig. 6.

(GaAs). Numerical results show that charge and spin transport characteristics of such a single junctions are highly asymmetrical and reveal features typical of charge and spin diodes.

We have also analyzed spin and charge transport in double-barrier heterostructures, Fe/MgO/GaAs/MgO/Fe. For these structures, two limiting situations were considered: (i) the limit of weak (negligible) spin relaxation in GaAs, when a spin accumulation builds up in the GaAs layer and (ii) the limit of fast spin relaxation in GaAs, when the GaAs layer thickness is larger than the spin relaxation length. In the former case, there is a remarkable tunnel magnetoresistance associated with transition from the antiparallel to parallel alignment of the electrodes' magnetizations. In the latter case, in turn, there is no spin accumulation in the GaAs layer, and also no tunnel magnetoresistance associated with transition from antiparallel to parallel magnetic configuration. This is because the spin memory is lost in the GaAs layer due to strong spin-flip scattering. Numerical results have been fitted to experimental data obtained on a two-barrier junction, and a satisfactory agreement of these data with numerical results has been achieved.

ACKNOWLEDGMENTS

This work is supported by the National Center of Research and Development in Poland in frame of EU project Era.Net.Rus "SpinBarrier."

[1]I. Žutic, J. Fabian, and S. Das Sarma, Rev. Mod. Phys. **76**, 323 (2004).
[2]J. Fabian, A. Matos-Abiague, C. Ertler, P. Stano, and I. Zutic, Acta Phys. Slovaca **57**, 565 (2007).
[3]W. Y. Lee, S. Gardelis, B. C. Choi, Y. B. Xu, C. G. Smith, C. H. W. Barnes, D. A. Ritchie, E. H. Linfield, and J. A. C. Bland, J. Appl. Phys. **85**, 6682 (1999).
[4]P. R. Hammar, B. R. Bennet, M. J. Yang, and M. Johnson, Phys. Rev. Lett. **83**, 203 (1999).
[5]G. Schmidt, D. Ferrand, L. W. Molenkamp, A. T. Filip, and B. J. van Wees, Phys. Rev. B. **62**, R4790 (2000).
[6]E. I. Rashba, Phys. Rev. B **62**, R16267 (2000).
[7]V. F. Motsnyj, P. Van Dorpe, W. Van Roy, E. Goovaerts, V. I. Safarov, G. Borghs, and J. De Boeck, Phys. Rev. B **68**, 245319 (2003).
[8]G. Salis, R. Wang, X. Jiang, R. M. Shelby, S. S. P. Parkin, S. R. Bank, and J. S. Harris, Appl. Phys. Lett. **87**, 262503 (2005).
[9]X. Jiang, R. Wang, R. M. Shelby, R. M. Macfarlane, S. R. Bank, J. S. Harris, and S. S. P. Parkin, Phys. Rev. Lett. **94**, 056601 (2005).
[10]X. Lou, C. Adelmann, S. A. Crooker, E. S. Garlid, J. Zhang, K. S. Madhukar Reddy, S. D. Flexner, C. J. Palmstrøm, and P. A. Crowell, Nat. Phys. **3**, 197 (2007).
[11]Y. J. Park, M. C. Hickey, M. J. Van Veenhuizen, J. Chang, D. Heiman, C. H. Perry, and J. S. Moodera, J. Phys.: Condens. Matter **23**, 116002 (2011).
[12]S. M. Sze and K. K. Ng, *Physics of Semiconductor Devices* (John Wiley and Sons, Hoboken, 2007).
[13]J. G. Simmons, J. Appl. Phys. **34**, 1793 (1963).
[14]E. H. Rhoderick, IEE Proc. **129**(1), 1 (1982).
[15]H. Ikoma, T. Ishida, K. Sato, T. Ishikawa, and K. Maeda, J. Appl. Phys. **73**, 1272 (1993).
[16]A. M. Bratkovsky, Phys. Rev. B **56**, 2344 (1997).
[17]I. Zutic, J. Fabian, and S. Das Sarma, Phys. Rev. B **64**, 121201 (2001).
[18]A. Khaetskii, J. C. Egues, D. Loss, C. Gould, G. Schmidt, and L. W. Molenkamp, Phys. Rev. B **71**, 235327 (2005).
[19]A. N. Chantis and D. L. Smith, Phys. Rev. B **78**, 235317 (2008).
[20]W. H. Butler, X.-G. Zhang, T. C. Schulthess, and J. M. MacLaren, Phys. Rev. B **63**, 054416 (2001).
[21]J. Mathon and A. Umerski, Phys. Rev. B **63**, 220403(R) (2001).
[22]S. S. P. Parkin, C. Kaiser, A. Panchula, P. M. Rice, B. Hughes, M. Samant, and S.-H. Yang, Nature Mater. **3**, 862 (2004).
[23]S. Yuasa, T. Nagahama, A. Fukushima, Y. Suzuki, and K. Ando, Nature Mater. **3**, 868 (2004).
[24]L.-N. Tong, F. Matthes, M. Müller, C. M. Schneider, and C.-G. Lee, Phys. Rev. B **77**, 064421 (2008).
[25]T. Nickiel, "Structural, electrical and magnetic properties of iron layers grown on (001)GaAs," Ph.D. thesis (Universität Hamburg, 2012).